JURNAL GRADASI TEKNIK SIPIL Volume 9, No. 2, 2025 :170-185

ISSN 2598-975 (Print)
ISSN 2598-8581 (Online)
ejurnal.poliban.ac.id

BACK ANALYSIS OF SIX-STOREY BUILDING'S PILE FOUNDATION BEARING CAPACITY FAILURE

Femy Sarah Masyithah[1*], Helmy Darjanto[2]

[1,] *Department of Civil Engineering, Muhammadiyah University of Surabaya, Indonesia*
e-mail: **[*1]femy.sarah.masyithah-2020@ft.um-surabaya.ac.id** (*corresponding author*)

Abstrak

Penelitian ini mengkaji kegagalan kapasitas beban fondasi pada bangunan enam lantai, yang upaya mitigasinya dengan injeksi semen tidak berhasil. Analisis balik dilakukan menggunakan data penyelidikan tanah (log sumur bor, nilai SPT, dan uji laboratorium), uji beban statis (SLT), dan pengukuran Pile Driving Analyzer (PDA) untuk mengevaluasi ulang desain kelompok tiang dan sistem pondasi piled-raft yang diusulkan. Kapasitas aksial tiang dievaluasi dengan empat metode yang umum digunakan—API, Revised Lambda, USACE, dan FHWA—karena metode-metode ini mewakili praktik internasional dan Indonesia yang berlaku serta menjadi dasar analitis untuk SNI 8460:2017. Hasil analisis menunjukkan bahwa kelompok tiang yang ada tidak mampu menahan beban kerja yang diterapkan, dan sistem pondasi piled-raft yang diusulkan tidak memenuhi kriteria desain yang required. Analisis balik lebih lanjut menunjukkan bahwa, pada tanah permukaan yang sangat longgar, proporsi beban yang ditanggung oleh raft harus dibatasi sekitar 20% untuk menghindari overstressing tanah dan memicu penurunan tambahan. Studi ini berkontribusi pada pemahaman yang lebih baik tentang desain dan retrofit fondasi tiang-raft pada endapan granular longgar dengan menghubungkan perhitungan kapasitas berdasarkan kode dengan uji beban lapangan, serta memberikan panduan praktis untuk memeriksa pembagian beban antara tiang dan raft pada kondisi tanah lunak.

Kata kunci*— Analisis Balik, Kegagalan Daya Dukung, Piled Raft, Tiang Pancang*

Abstract

This study investigated the foundation bearing capacity failure of a six-storey building, which was unsuccessfully mitigated by cement injection. Back analysis was carried out using soil investigation data (borehole logs, SPT values, and laboratory tests), static load tests (SLT), and pile driving analyzer (PDA) measurements to reassess the design of the pile group and the proposed piled-raft system. The axial capacity of the piles was evaluated with four commonly used methods—API, Revised Lambda, USACE, and FHWA—because they represent prevailing international and Indonesian practice and form the analytical basis for SNI 8460:2017. The analysis results revealed that the existing pile group was unable to withstand the applied working loads, and that the proposed piled raft did not satisfy the required design criteria. The back analysis further showed that, in very loose surface soils, the proportion of load carried by the raft should be limited to approximately 20% to avoid overstressing the soil and triggering additional settlement. This study contributes to a better understanding of the design and retrofit of piled-raft foundations in loose granular deposits by linking code-based capacity calculations with field load tests and by providing practical guidance for checking load sharing between piles and raft in soft ground conditions.

Keywords—*Back Analysis, Bearing Capacity Failure, Pile Foundation, Piled Raft*

I. INTRODUCTION

In geotechnical engineering, foundation failures pose significant risks to building safety and serviceability. Design codes such as the Indonesian National Standard SNI 1729:2019 require that foundations remain stable and that failure does not occur before the overlying structure, highlighting the need for reliable foundation systems in seismic and non-seismic regions. Pile foundations are widely used for multi-storey buildings to transfer axial and lateral loads to deeper, more competent soil layers. In practice, ground improvement methods such as cement injection or

History of article:
Received : 06 Juni 2024
Revised : 28 November 2025
Published : 31 Desember 2025

ISSN 2598-975 (Print)
ISSN 2598-8581 (Online)
ejurnal.poliban.ac.id

grouting are often adopted to mitigate bearing capacity and settlement problems in marginal soils (Li et al., 2024). However, these measures do not always prevent failure.

A critical example is a six-storey building in Dili City, Timor Leste, where the pile foundation exhibited excessive settlement of up to approximately 400 mm and indications of bearing capacity failure, even after remedial cement injection works had been carried out. This case highlights a lack of integration between the original pile group design and the concept of piled-raft foundations, and it raises questions about the adequacy of conventional design checks and repair strategies for loose, heterogeneous deposits in coastal urban areas.

Piled-raft foundations have been widely investigated through analytical, numerical, and experimental studies. These studies demonstrate that allowing both the raft and the piles to share the applied load can increase overall stiffness, control differential settlement, and reduce demands on individual piles. Recent works have also shown the usefulness of back analysis of load tests to reassess pile capacities and foundation performance. Nevertheless, relatively few studies report detailed back analysis of a failed pile foundation together with a proposed piled-raft retrofit, especially under local soil conditions similar to those in Dili.

This study addresses that gap by using back analysis of soil investigation data, static load tests, and pile driving analyzer (PDA) measurements to evaluate both the existing pile foundation and a proposed piled-raft system for the Dili building. The analysis links code-based capacity calculations according to SNI 8460:2017 with field performance, and examines how load sharing between the raft and piles should be controlled in very loose surface soils to avoid renewed failure.

Therefore, the objectives of this study are (1) to identify the causes of bearing capacity failure of the existing pile foundation system for the six-storey building in Dili, and (2) to evaluate the design adequacy and load-sharing behaviour of the proposed piled-raft foundation based on comprehensive back analysis of the available field and laboratory data.

The remainder of this paper is organized as follows. Section II describes the research methodology, including the project background, site investigation programme, and back-analysis procedure. Section III presents and discusses the results of the capacity evaluations and load-sharing analyses for the pile group and piled-raft system. Section IV summarizes the main findings and provides practical recommendations for the design and retrofit of piled-raft foundations in similar soil conditions.

A. Rational Design of Piled Raft

The findings emphasize the importance of rational pile foundation design, based on collaboration between rafts and piles to increase their overall stiffness and capacity, control differential settlement, and reduce stress states in pile and raft foundations. This research also highlights the need for special analysis when the applied load distribution is not uniform. In addition, it is suggested that for piled rafts designed according to a particular approach, the axial load on the piles should be as high as 80% or more of their geotechnical resistance under working load conditions. This also emphasizes the importance of considering piles as structural elements that should be designed appropriately. The use of piled-raft foundations must consider the distribution of the load carried by rafts which is very dependent respectively on the area of the pile group and raft, the diameter of the pile, and the distance between the piles as well as the consistency of the surface soil as in Figure 1.

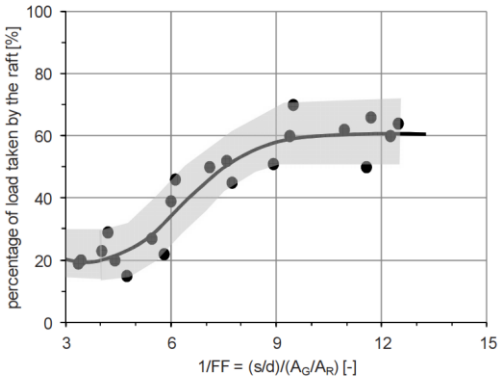

Figure 1. Percentage of load taken by the raft: experimental data collected (Mandolini et al., 2013).

B. Piled Raft Capacity Requirement (Febriansya et al., 2022)

The results of the study showed that piled-raft foundations are a suitable alternative for buildings with large loads on lens soil conditions. The foundation was designed with a raft thickness of 1.6 meters and a bored pile diameter of 1.2 meters at a depth of 35 meters. The raft has a bearing capacity of 54.251 kN/m^2 and the bored pile group has a bearing capacity of 468,628.285 kN/m^2 with 220 piles 3 meters apart. The raft withstands 18.152% of the total load, while the bored pile withstands 81.848%. The foundation meets the strength and settlement requirements, with a total settlement of 21.923 mm, which is less than the maximum allowable settlement of 150 mm. The analysis shows that the piled-raft foundation meets the strength and usability requirements of SNI 8460:2017.

C. Pile-Raft Interaction

Important insights into piled-raft behavior have come from parametric studies by Randolph (1994), Poulos (2001), and Katzenbach et al. (1998). There are many intricate interactions going on between the many components of a piled raft. The way that various parts of a piled-raft interact with one another is described below by Burland et al., 2012.

1) *Raft–soil interaction:* The contact pressures that are imparted into the soil between the raft and the soil cause the raft to settle.

History of article:
Received : 06 Juni 2024
Revised : 28 November 2025
Published : 31 Desember 2025

ISSN 2598-975 (Print)
ISSN 2598-8581 (Online)
ejurnal.poliban.ac.id

2) *Raft–soil–raft interaction:* Interaction between the soil and other raft components occurs.
3) *Raft–soil–pile interaction:* Through the soil, the raft contact stresses communicate with the piles.
4) *Raft–pile interaction:* The raft directly transfers loads into the piles.
5) *Pile–soil interaction:* The loads in the pile dispersed throughout the surrounding soil.
6) *Pile–soil–pile interaction:* Through the earth, interactions occur between each pile and other piles.
7) *Pile–soil–raft interaction:* Through the soil, there is additional interaction between each pile and the underside of the raft.

To understand the piled-raft foundation well, first, consider the foundation system that receives the total structure load (V_{PR}) and the ratio between single pile load and V_{PR} (α_{PR}). A load-sharing ratio $\alpha_{PR} = 0$ represents a shallow foundation with no piles, while $\alpha_{PR} = 1$ represents a pile group with a raft not in contact with the ground, and piled-raft foundations cover the range $0 < \alpha_{PR} < 1$.

The PDR method (Poulos, Davis, and Randolph) is widely used for piled-raft foundation applications. In principle, the friction resistance of the pile foundation begins to be mobilized and the raft is in elastic condition. Ultimate capacity; the vertical bearing capacity can be taken as the lesser of:

- the block's capacity, which includes the raft's portion outside the pile-group boundary as well as the piles and raft.
- the calculated maximum capacity of the piles and the raft combined, as shown by Equation 1.

Equation 1. Factored Ultimate Capacity.

$$Q_{PR} = \alpha_P Q_P + \alpha_R Q_R \quad (1)$$

where,
$\alpha_{R/P}$ = load ratio between raft/pile,
$Q_{R/P}$ = ultimate capacity of raft/pile.

According to Mandolini et al. (2005) pile-group block failure is probably to occur for small pile spacing values, below S_{crit}, with S_{crit}/d varying between 2.5 (for 3×3 pile groups) and 3.5 (for 9×9 piles group) where d is the pile diameter. The ultimate geotechnical capacity of the piled-raft, Q_{PR}, can be used for pile spacing greater than S_{crit}.

D. Foundation Failures and Piled-Raft Application

Foundation failures in multi-storey buildings are frequently linked to weak or heterogeneous soils and to foundation systems that do not adequately control settlement. Piled-raft foundations have emerged as an efficient alternative because they combine the advantages of rafts and pile groups and can support heavier loads than either system alone, particularly under challenging soil conditions. Piled rafts have been successfully applied to high-rise buildings and other large structures, and that their performance is governed by the load-sharing mechanism between the raft and the piles (Mudher et al., 2025)

In that review, the load-sharing ratio is identified as a key design parameter that depends on pile spacing and arrangement, settlement level, loading conditions, pile length, and soil friction angle. The interaction is non-linear: conventional designs that ignore raft contribution tend to be uneconomical, while overestimating the raft share can be unsafe. Field monitoring of piled foundations on soft clay indicates that, even when the raft is neglected in design, it may still carry about 10–20% of the total load. However, detailed case histories in which a failed pile foundation is re-evaluated and retrofitted using a piled-raft system remain limited. This study contributes to that gap by using back analysis of a real failure case to assess a piled-raft solution and to examine an appropriate range of raft load share under local loose soil conditions in Dili.

E. Liquefaction Analysis

According to Hakam (2020), liquefaction is an event that changes the condition of the soil from solid to liquid. Liquefaction is often found in earthquakes where soil behavior occurs due to earthquake loads that occur only in a short time. Earthquake vibrations that propagate in soil deposits in a short time cause the soil mass to transition from a solid state (behavior) to a liquid state (liquid behavior). Most liquefaction occurs when D_{50} lies in the range of 0.1-1 mm. Liquefaction potential analysis methods continue to be developed with data enrichment from events. To analyze the liquefaction potential of a site, the following steps can be taken:

First, conduct a geotechnical investigation at the site to obtain key soil parameters at specific depths. The investigation is carried out using a machine drill so that it can reach depths of up to 30 m from the ground surface. During the investigation, disturbed and native (undisturbed) samples are taken. Usually, a deep boring investigation will also be followed by standard penetration testing to obtain N_{SPT} values. This data will be required for various construction activities.

Secondly, disturbed soil samples at a certain depth are tested in the laboratory using sieve analysis to obtain the grain size distribution of the soil to obtain the D_{50} parameter. The disturbed soil can also be used for maximum and minimum volume weight testing. The original soil sample, on the other hand, is tested for its volume weight, and moisture content.

Once the parameters D_{50} and D_r are obtained, they are plotted onto the liquefaction diagram created from the laboratory testing results and liquefaction data comparison. If the D_{50}-D_r intersection point is to the left of the acceleration limit line, then the soil layer at that point has the potential to liquefy during an earthquake and vice versa. The value of the acceleration limit can be determined from the Earthquake Acceleration Map at the location investigated with SNI 8460:

History of article:
Received : 06 Juni 2024
Revised : 28 November 2025
Published : 31 Desember 2025

2017. The MCEG peak acceleration value adjusted for site effect (PGAM) is the one used for the evaluation of liquefaction and other geotechnical problems.

The procedure for analyzing liquefaction potential based on average grain size and relative density can be outlined in the flow chart shown in Figure 2.

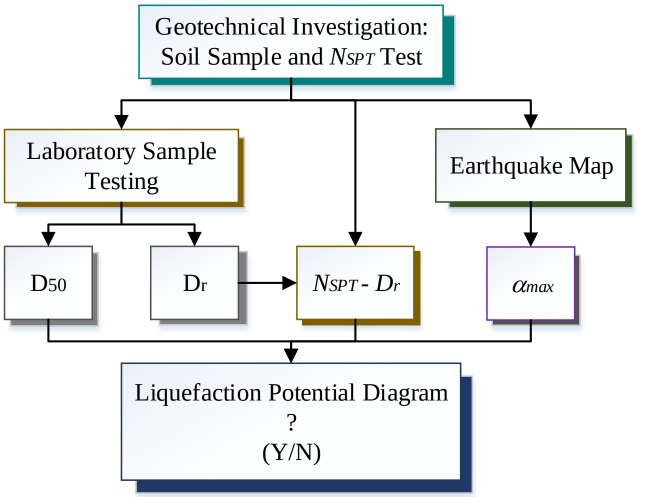

Figure 2. Practical Analysis Procedure of Liquefaction Potential (Hakam, 2020).

II. RESEARCH METHOD

A. Research Flow and Overall Approach

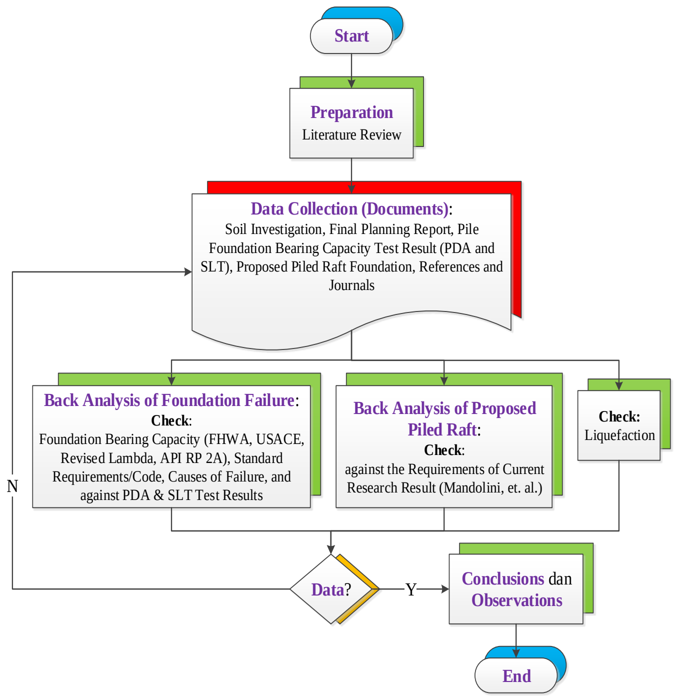

Figure 3. Research flowchart.

This study was designed as a back-analysis of a failed pile foundation and a proposed piled-raft retrofit for a six-storey building in Dili, Timor Leste. The overall research flow is summarized in the flowchart in Figure 3 and can be described in five main stages:

1) ***Preparation and literature review:*** Relevant design codes (API RP 2A, FHWA, USACE, SNI 8460:2017) and previous studies on piled-raft behaviour and back-analysis of pile foundations were reviewed to define the research problem, formulate the hypotheses, and select appropriate analytical methods.
2) ***Data collection:*** Project documents were compiled, including soil investigation reports (borehole logs, NSPT values, laboratory test results) from two boreholes located in the same geomorphological unit as the project site, the original foundation design calculations and drawings, static load test (SLT) reports for two test piles, pile driving analyzer (PDA) test data, and the proposed piled-raft foundation design prepared as a remedial option.
3) ***Derivation of geotechnical parameters:*** From the soil investigation data, stratigraphic profiles and design parameters were established for each layer: saturated and effective unit weights (γ_{sat}, γ'), undrained shear strength C_u (for fine-grained soils), friction angle φ' (for coarse-grained soils), earth pressure coefficient K_0, and bearing capacity factor N_q. For sand and gravel layers, correlations between N_{SPT} and relative density were used to estimate φ' and N_q, while adhesion factors α were obtained following the recommendations of API, FHWA, and USACE for bored piles. Negative skin friction in the very loose upper layers ($N_{SPT} < 5$) was explicitly included in the axial capacity calculations.
4) ***Back analysis of the existing pile foundation:*** Using the derived soil parameters and the actual pile geometry, the ultimate axial capacity profile of single piles was computed along depth for each method (API, FHWA, USACE, Revised Lambda). For every method and each borehole, the unit shaft resistance and end-bearing resistance were integrated to obtain the ultimate capacity, and then compared with the measured ultimate loads from SLT and PDA. The level of agreement between calculated and measured capacities was used to evaluate the adequacy of each method for the local soil conditions. In this study, the back analysis was carried out as a comparison exercise without iterative optimization: input parameters were kept within the ranges supported by field and laboratory data, and no arbitrary calibration outside code-recommended values was applied.
5) ***Evaluation of the proposed piled-raft system:*** Once the axial capacity of single piles had been established, the pile group capacity was assessed considering group efficiency and pile–pile interaction. The bearing capacity and settlement of the raft were then evaluated based on SNI 8460:2017 using the shallow foundation bearing capacity equations and an elastic settlement approach. Several

History of article:
Received : 06 Juni 2024
Revised : 28 November 2025
Published : 31 Desember 2025

ISSN 2598-975 (Print)
ISSN 2598-8581 (Online)
ejurnal.poliban.ac.id

load-sharing scenarios between raft and piles were examined. The proposed piled-raft configuration was checked against axial capacity and settlement limits in SNI 8460:2017, and piled-raft performance criteria from Mandolini et al., for acceptable raft load share and settlement control.

B. Research Location

The site lies on the coastal plain of Dili, on the eastern tip of Timor Island, which forms part of the Outer Non-Volcanic Banda Arc. The regional geology is characterized by complex tectonostratigraphic units (Allochthon/Banda Terrane, para-autochthonous units, and autochthonous sediments) resulting from the collision between the Banda Arc and the Australian continental margin.

Morphologically, the area exhibits steep slopes in the hinterland and extensive alluvial fans and floodplains along the coastal zone. The research site is situated on these young alluvial deposits, consisting predominantly of sand and gravel with interbedded silt layers and a shallow groundwater table. The steep equilibrium, with almost half of Timor's land having a slope of 40° or more, has prevented the development of classic soil profiles (Thompson, 2011). Figure 4 shows the location of the building within the urban fabric of Dili, while Figure 5 illustrates the site conditions at the time of investigation.

Figure 4. Research Location (*Source: Google Earth*).

Figure 5. Conditions at the Research Site.

C. Soil Data

Subsurface conditions were derived from two boreholes (Borehole #1 and Borehole #2) located in the same alluvial fan system as the project site. Due to security restrictions at the project, direct drilling at the exact building location was not permitted; therefore, the available boreholes are situated in nearby open areas with similar topography and geomorphology.

Standard penetration tests (SPT) were performed at regular depth intervals, and disturbed and undisturbed samples were taken for classification and laboratory testing. Both boreholes show very loose sand and gravel in the upper 4–5 m ($N_{SPT} <$ 5), underlain by loose to medium-dense sand and gravel and, at greater depth, dense sand and gravel layers. The NSPT values, soil types, unit weights, strength parameters, and bearing capacity factors for each layer are summarized in

TABLE **1** (Borehole #1) and

TABLE **2** (Borehole #2).

Using these data, soil layers were grouped into representative strata for design purposes. For each stratum, the following parameters were defined for input into the analytical models:

1) γ_{sat} and γ': from laboratory unit weight and groundwater depth,
2) C_u: for cohesive layers (from laboratory shear tests),
3) φ': for granular layers (from laboratory tests and $N_{SPT} - \varphi'$ correlations),
4) K_0: from empirical correlations based on soil type and overconsolidation, and
5) $N_q and \ \alpha$: from API, FHWA, and USACE recommendations.

Because the boreholes are located near, but not exactly at, the building footprint, this introduces uncertainty in the representation of the actual soil profile at the project site. To address this limitation, a simple parametric sensitivity analysis was performed by varying key soil parameters (φ' and C_u) within realistic ranges (±2–3° for φ' and ±20% for C_u) and recomputing the axial capacity of single piles. The results showed that while the absolute values of capacity changed, the qualitative conclusions regarding failure of the existing pile group and the inadequacy of the proposed piled

History of article:
Received : 06 Juni 2024
Revised : 28 November 2025
Published : 31 Desember 2025

ISSN 2598-975 (Print)
ISSN 2598-8581 (Online)
ejurnal.poliban.ac.id

raft remained unchanged. In addition, the comparison with SLT and PDA test results provided an indirect calibration of the adopted soil parameters for the depth range where tests were performed.

TABLE 1. Soil Data for Borehole #1

No.	Depth (m)	DH (m)	Soil Type and Consistency	N_{SPT}	γ_{sat} (kN/m^3)	γ' (kN/m^3)	C_u (kPa)	φ (°)	K_0	N_q	α
1	4	4	very loose silt	1	15.7	5.7	6	-	-	-	1
2	5	1	very loose sand	1	15.7	5.7	-	23.464	0.602	8	-
3	6	1	medium dense gravel	21	20.5	10.5	-	35.875	0.414	32	-
4	7	1	loose sand	7	17.25	7.25	-	29.165	0.513	12	-
5	9	2	very loose gravel	4	19	9	-	26.928	0.547	12	-
6	10	1	dense gravel	49	21	11	-	44.249	0.302	40	-
7	20	10	loose gravel	8	20	10	-	29.798	0.503	12	-
8	22	2	very dense gravel	50	21	11	-	44.495	0.299	50	-
9	25	3	medium dense sand	20	18.85	8.85	-	35.492	0.419	32	-
10	27	2	medium dense silt	22	20	10	132	-	-	-	0.5
11	30	3	medium dense sand	26	19.78	9.78	-	37.664	0.389	37	-
12	35	5	dense sand	50	22	12	-	44.495	0.299	40	-

TABLE 2. Soil Data for Borehole #2

No.	Depth (m)	DH (m)	Soil Type and Consistency	N_{SPT}	γ_{sat} (kN/m^3)	γ' (kN/m^3)	C_u (kPa)	φ (°)	K_0	N_q	α
1	2	2	very loose sand	1	15.7	5.7	-	23.464	0.602	8	-
2	4	2	loose sand	10	19.6	9.6	-	30.954	0.486	20	-
3	8	4	medium dense sand	15	18.075	8.075	-	33.416	0.449	32	-
4	10	2	medium dense gravel	21	20	10	-	35.875	0.414	32	-
5	12	2	very loose gravel	4	19	9	-	26.928	0.547	12	-
6	14	2	very loose silt	1	16	6	6	-	-	-	1
7	16	2	loose silt	7	16.5	6.5	42	-	-	-	0.81
8	18	2	very loose silt	1	16	6	6	-	-	-	1
9	19	1	loose silt	7	16.5	6.5	42	-	-	-	0.81
10	21	2	very loose gravel	2	19	9	-	24.899	0.579	9	-
11	24	3	loose gravel	10	19.5	9.5	-	30.954	0.486	20	-
12	27	3	medium dense gravel	17	20	10	-	34.283	0.437	32	-
13	29	2	dense sand	39	19.415	9.415	-	41.633	0.336	40	-
14	31	2	dense gravel	43	20	10	-	42.716	0.322	40	-
15	33	2	dense sand	31	17.535	7.535	-	39.287	0.367	40	-
16	35	2	very dense sand	50	22	12	-	44.495	0.299	40	-

History of article:
Received : 06 Juni 2024
Revised : 28 November 2025
Published : 31 Desember 2025

ISSN 2598-975 (Print)
ISSN 2598-8581 (Online)
ejurnal.poliban.ac.id

D. Back Analysis Procedure

The back analysis in this study consisted of three main components:

1) ***Single-pile capacity evaluation:***

For each borehole, the axial capacity of a single bored pile was computed using:

- **API RP 2A-WSD**: α-method for shaft resistance in clays and β/q–z correlations for sands, with end bearing based on N_q;
- **FHWA**: layer-by-layer evaluation using NSPT-based correlations for unit shaft friction and end bearing for bored piles;
- **USACE**: empirical correlations for shaft resistance and end bearing for bored piles in granular and cohesive soils;
- **Revised Lambda method**: elastic continuum approach using a λ-factor to relate pile displacement and load transfer along the shaft and at the base.

For each method, the total skin friction, end-bearing resistance, and negative skin friction were integrated along pile length to produce capacity–depth curves. These were then compared to the measured ultimate loads from SLT and PDA. Agreement within a reasonable engineering range (approximately ±20% of the measured ultimate capacity) was considered acceptable.

2) ***Pile group and piled-raft evaluation:***

Using the capacities derived in Step 1, the pile group capacity was evaluated including group efficiency factors based on pile spacing and arrangement. The raft bearing capacity and settlement were computed using SNI 8460:2017 and conventional elastic settlement theory, accounting for the very loose near-surface soils. Several load-sharing ratios between raft and piles were analysed to identify the maximum allowable raft share that kept:

- the contact pressure under the raft below the ultimate bearing capacity of the upper layers, and
- the total settlement and differential settlement within the serviceability limits recommended by SNI 8460:2017 and Mandolini et al., (2013).

3) ***Consistency check and convergence criterion***

Although no iterative numerical optimization was performed, the back analysis was considered converged when three conditions were simultaneously satisfied:

- the calculated ultimate capacity of single piles from at least one method fell within the acceptable range of the SLT and PDA results;
- the pile group and piled-raft system met strength and settlement criteria under the design loads; and
- sensitivity analyses on ϕ′ and Cu did not change the qualitative conclusion that the original pile group was inadequate and that the piled raft required limiting the raft load share to about 20% in the very loose upper soils.

E. Design Codes, Empirical Methods, and Their Applicability

Four empirical/analytical methods were adopted (API, FHWA, USACE, Revised Lambda) because they:

- are widely used in international practice for axial pile capacity evaluation;
- form the analytical basis for the implementation of SNI 8460:2017 in Indonesia; and
- cover both granular and cohesive soils as encountered at the Dili site.

In this case study, the methods were applied with the following considerations and limitations:

- **API RP 2A-WSD** is primarily developed for offshore piles, typically driven piles in sand and clay; here it was applied to bored piles with caution, using conservative adhesion factors and end-bearing coefficients.
- **FHWA** guidance is oriented to onshore drilled shafts and driven piles; it is suitable for the bored piles in this project, but the correlations are based on NSPT data and may be less accurate in very loose sands (NSPT < 5), which is one reason negative skin friction was included explicitly.
- **USACE** procedures provide an additional empirical check, especially for military and infrastructure projects, but are also empirical and sensitive to local calibration.
- The **Revised Lambda method** provides an analytical framework for load transfer and settlement of piles and piled rafts, but assumes linear-elastic soil behaviour within the working load range and may not fully capture non-linearities in very loose surface deposits.

All standards and design documents (API RP 2A-WSD, FHWA, USACE manuals, and SNI 8460:2017) are cited in the reference list with full bibliographic details, and their use is limited to the ranges of soil type, pile type, and loading conditions for which they are intended.

III. RESULT AND DISCUSSION

A. Calculation of Allowable and Ultimate Bearing Capacity of Pile Foundation

Based on the soil parameters derived in the previous section, the ultimate and allowable axial capacities of the bored piles were calculated for Borehole #1 and Borehole #2. The layer-by-layer values of unit shaft resistance, end bearing, and negative skin friction are summarized in TABLE 3 and TABLE 4. The results show that the total ultimate capacity increases significantly once the piles penetrate the deeper dense sand and gravel layers, while the contribution from the very loose surface soils (NSPT < 5) is small and dominated by negative skin friction.

Overall, the calculated allowable capacities of the single piles remain lower than the design working load used in the original foundation plan, especially when realistic safety factors and deformation limits are applied. This confirms that the original pile design did not provide an adequate margin of safety, even before considering pile-group interaction and construction uncertainties.

History of article:
Received : 06 Juni 2024
Revised : 28 November 2025
Published : 31 Desember 2025

ISSN 2598-975 (Print)
ISSN 2598-8581 (Online)
ejurnal.poliban.ac.id

TABLE 3. Calculation of Ultimate and Allowable Bearing Capacity for Borehole #1

No.	f_s (kPa)	f_p (kPa)	Q_s (kN)	ΣQ_s (kN)	Q_p (kN)	Q_{ult} (kN)	SF	Q_{all} (kN)	Q_{all} (ton)	Depth (m)
1	6	54	30.159	30.159	6.786	36.945	2.5	14.778	1.478	4
2	2	40	2.513	32.673	5.027	37.699	2.5	15.080	1.508	5
3	42	840	52.779	85.451	105.558	191.009	2.5	76.404	7.640	6
4	14	280	17.593	103.044	35.186	138.230	2.5	55.292	5.529	7
5	8	160	20.106	123.150	20.106	143.257	2.5	57.303	5.730	9
6	98	16000	123.150	246.301	2010.619	2256.920	2.5	902.768	90.277	10
7	16	320	201.062	447.363	40.212	487.575	2.5	195.030	19.503	20
8	100	16000	251.327	698.690	2010.619	2709.310	2.5	1083.724	108.372	22
9	40	800	150.796	849.487	100.531	950.018	2.5	380.007	38.001	25
10	66	1188	165.876	1015.363	149.288	1164.651	2.5	465.860	46.586	27
11	52	1040	196.035	1211.398	130.690	1342.088	2.5	536.835	53.684	30
12	100	16000	628.319	1839.717	2010.619	3850.336	2.5	1540.134	154.013	35

TABLE 4. Calculation of Ultimate and Allowable Bearing Capacity for Borehole #2

f_s (kPa)	f_p (kPa)	Q_s (kN)	ΣQ_s (kN)	Q_p (kN)	Q_{ult} (kN)	SF	Q_{all} (kN)	Q_{all} (ton)	Depth (m)
2	40	5.027	5.027	5.027	10.053	2.5	4.021	0.402	2
20	400	50.265	55.292	50.265	105.558	2.5	42.223	4.222	4
30	600	150.796	206.088	75.398	281.487	2.5	112.595	11.259	8
42	840	105.558	311.646	105.558	417.204	2.5	166.881	16.688	10
8	160	20.106	331.752	20.106	351.858	2.5	140.743	14.074	12
6	54	15.080	346.832	6.786	353.618	2.5	141.447	14.145	14
34.1	378	85.670	432.502	47.501	480.003	2.5	192.001	19.200	16
6	54	15.080	447.582	6.786	454.368	2.5	181.747	18.175	18
34.1	378	42.835	490.417	47.501	537.918	2.5	215.167	21.517	19
4	80	10.053	500.470	10.053	510.523	2.5	204.209	20.421	21
20	400	75.398	575.869	50.265	626.134	2.5	250.454	25.045	24
34	680	128.177	704.045	85.451	789.497	2.5	315.799	31.580	27
78	1560	196.035	895.054	196.035	1091.090	2.5	436.436	43.644	29
86	16000	216.142	1060.930	2010.619	3071.550	2.5	1228.620	122.862	31
62	1240	155.823	1065.957	155.823	1221.780	2.5	488.712	48.871	33
100	16000	251.327	1211.727	2010.619	3222.346	2.5	1288.938	128.894	35

History of article:
Received : 06 Juni 2024
Revised : 28 November 2025
Published : 31 Desember 2025

Comparisons of compressions and tensions taken from the computer results for each method can be seen in Figure 6, Figure 7, Figure 8, and Figure 9 for Borehole #1, and Figure 10, Figure 11, Figure 12, and Figure 13 for Borehole #2.

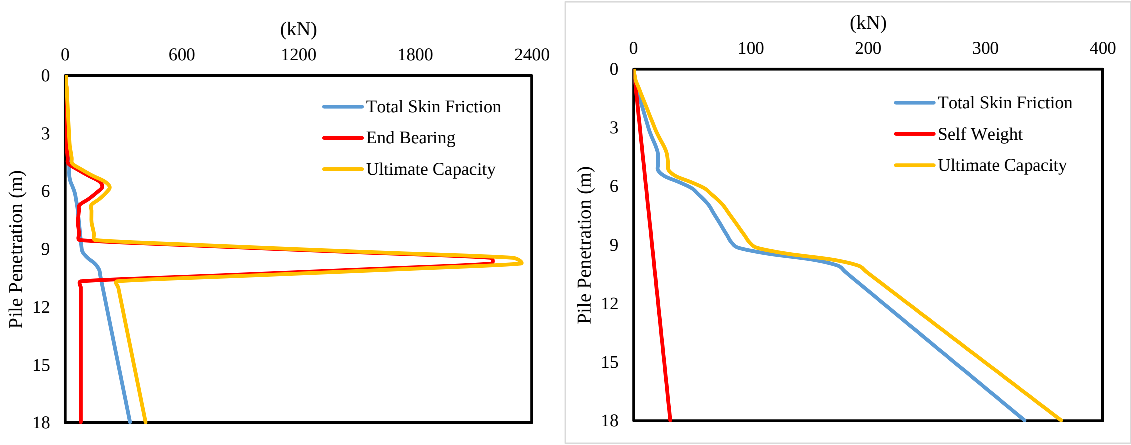

Figure 6. Comparison of Compression and Tension for FHWA Method in Borehole #1.

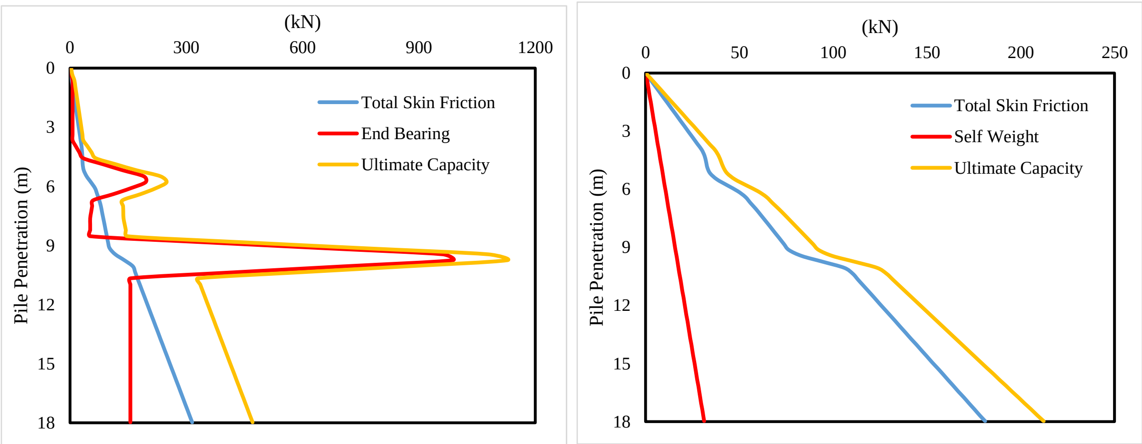

Figure 7. Comparison of Compression and Tension for Army Corps Method in Borehole #1.

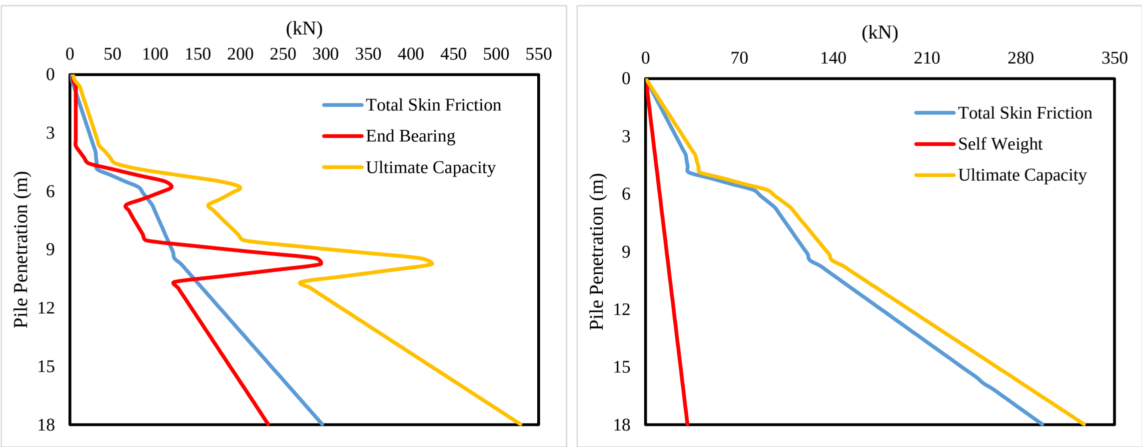

Figure 8. Comparison of Compression and Tension for Revised Lambda Method in Borehole #1.

ISSN 2598-975 (Print)
ISSN 2598-8581 (Online)
ejurnal.poliban.ac.id

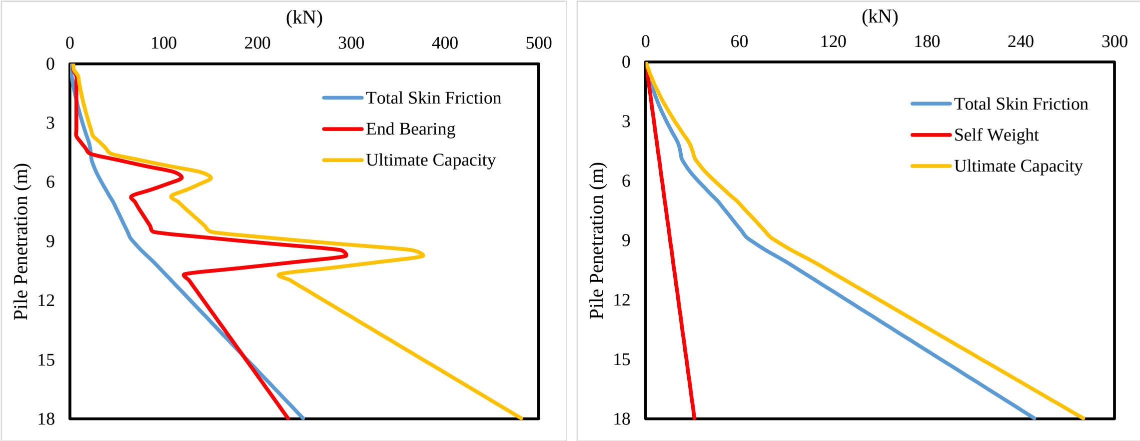

Figure 9. Comparison of Compression and Tension for API Method in Borehole #1.

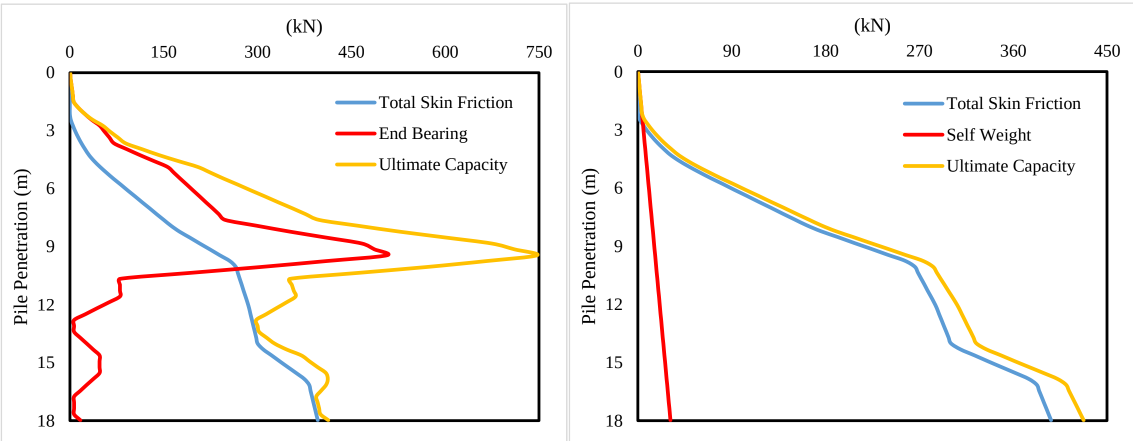

Figure 10. Comparison of Compression and Tension for FHWA Method in Borehole #2.

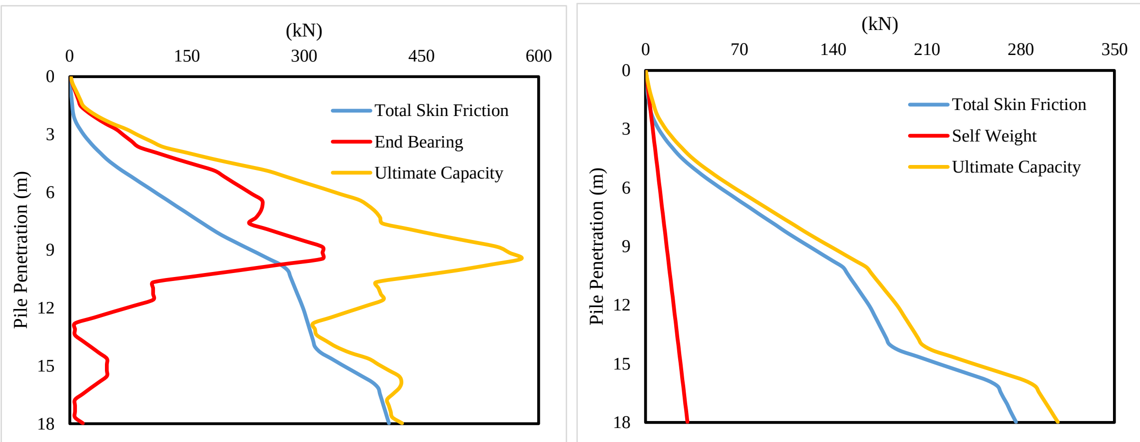

Figure 11. Comparison of Compression and Tension for Army Corps Method in Borehole #2.

History of article:
Received : 06 Juni 2024
Revised : 28 November 2025
Published : 31 Desember 2025

ISSN 2598-975 (Print)
ISSN 2598-8581 (Online)
ejurnal.poliban.ac.id

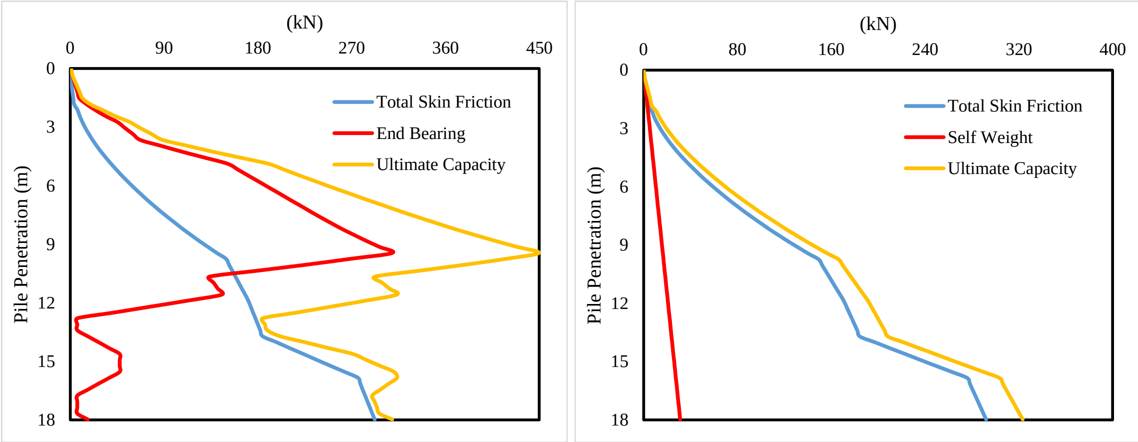

Figure 12. Comparison of Compression and Tension for Revised Lambda Method in Borehole #2.

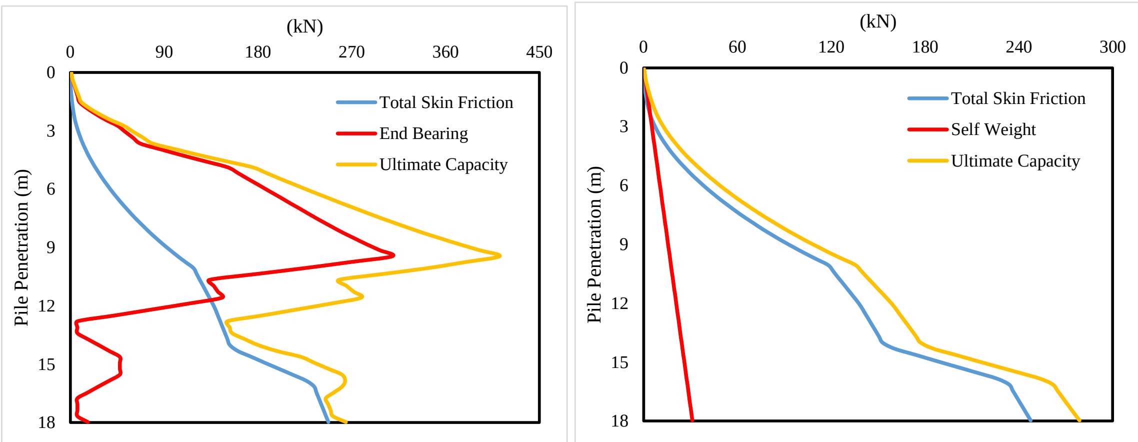

Figure 13. Comparison of Compression and Tension for API Method in Borehole #2.

The results of the above APILE program are summarized in

TABLE 5 below:

TABLE 5 Ultimate Axial Bearing Capacity of Piles

Item	BH-01	BH-02	SLT
Axial – Compression (kN)	486	243	450
Axial – Tension (kN)	286	258	-

In general, the API and FHWA methods give the lowest capacities, whereas the USACE and Revised Lambda methods predict higher capacities, closer to the field test results.

This trend can be explained by the basic assumptions of the methods. API and FHWA adopt relatively conservative unit shaft friction factors and reduction factors for bored piles in sand, and they effectively assign very low or zero positive shaft resistance in the very loose surface layers where NSPT < 5. As a consequence, the total capacity is governed by the deeper dense layers and is significantly reduced when negative skin friction is included. In contrast, the USACE and Revised Lambda methods allow higher mobilization of shaft resistance and end bearing in granular soils, leading to larger ultimate capacities. Since the evaluation is performed at single-pile level, pile spacing and group efficiency do not directly affect the differences between the four methods; these factors are considered later at the pile-group stage and applied consistently to all methods.

B. *SLT Test, PDA Test, and Calculation Results*

Referring to the Kronologia Problema Report, the ultimate bearing capacity of the pile foundation (Q_{ult}) from the static load test (SLT) is 450 kN and 900 kN (see TABLE 6), then if the safety factor for the compressive axial loading test on the pile foundation, SF = 2, then the bearing capacity of the pile foundation permit (Q_{all}) is $Q_{all} = Q_{ult}/2 = 450/2 = 225$ kN (say equivalent 22.5 tons) and $Q_{all} = 900/2 = 450$ kN with a note that it must be noted that the deformation limit at 200% of the plan loading.

History of article:
Received : 06 Juni 2024
Revised : 28 November 2025
Published : 31 Desember 2025

ISSN 2598-975 (Print)
ISSN 2598-8581 (Online)
ejurnal.poliban.ac.id

TABLE 6. Summary of Vertical Compressive Static Load Test (SLT) on Single Pile (Dia. 400 mm) (Kronologia Problema Report, 2021)

Sequence No.	Pile Serial No.	Pile Length (m)	Axial Ultimate Bearing Capacity (kN)	Settlement (mm)	Residual Settlement (mm)	The Ratio for Rebound of Settlement (%)
1	33	18	900	3.62	1.44	60.2
2	168	18	450	1.33	0.66	50.4

Furthermore, from the results of the Structure Analysis Report he bearing capacity of the pile foundation design (dia. 400 mm, depth: 18 m) $Q_{all} \geq 1000$ kN (109 tons, Ref.: Structure Analysis Report) was obtained, and the test results in the field were obtained, $Q_{all} = 225$ kN (smaller or ≤ 1000 kN). Then with the situation of the ability of the foundation of the pile group < from the working load, it is proposed to use rafts to overcome these conditions. In the project area, the consistency of surface soil up to -4.00 m is very loose silt (ML) so the contribution of raft-bearing capacity is not significant. Therefore, it is necessary to limit the percentage of load that can be carried by the ground under the raft area by a maximum of 20%.

C. Liquefaction Check

Figure 14 below are the results of the Grain Size Analysis. At the average diameter of D_{50}, it can be seen that the curve mostly does not fall within the range of 0.1-1 mm, so the site may be at low risk of liquefaction in the event of an earthquake. Another possibility is that there is no liquefaction damage if the piles are pre-cast or in situ within 45-60 feet long than as per site analysis.

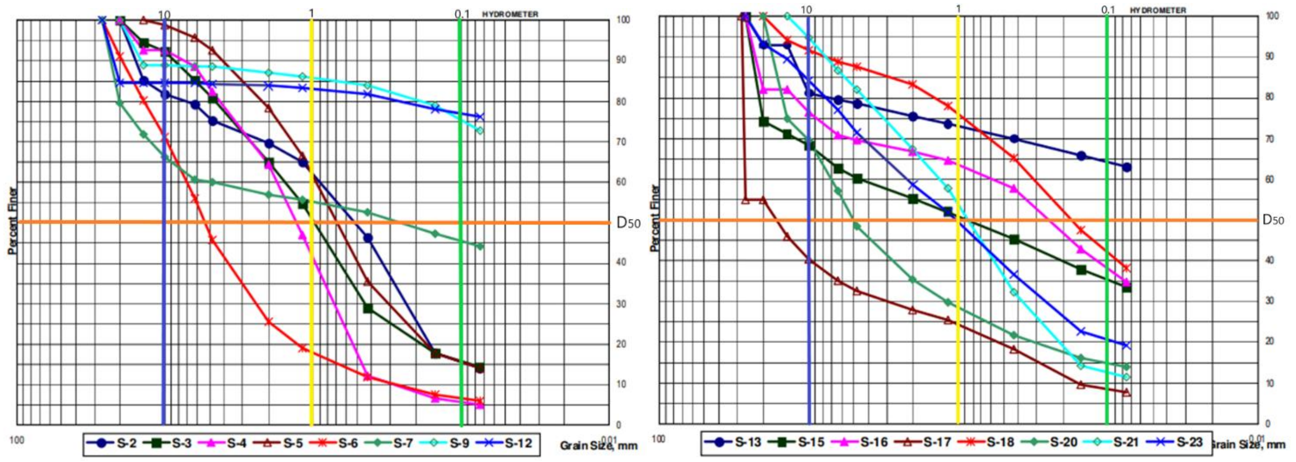

Figure 14. Grain Size Analysis on Plate-8 and Plate-9 (Structure Analysis Report, 2014).

D. Back Analysis of Bearing Capacity Failure

The APILE program was used to perform back analysis of the existing pile foundation by implementing the four methods (API, FHWA, USACE, Revised Lambda) as depth-dependent load-transfer models. This allowed the computed ultimate capacities to be compared directly with the SLT and PDA measurements for the actual pile geometry.

The back analysis shows that, when realistic soil parameters and negative skin friction in the very loose surface layer are considered, the allowable capacity of the pile group is significantly lower than the design working load. Even if the higher capacities predicted by the USACE and Revised Lambda methods are adopted, the pile group still does not reach the required capacity of ≥ 1000 kN per pile used in the structural design. The discrepancy arises from a combination of optimistic assumptions in the original design (ignoring negative skin friction and overestimating shaft resistance in loose layers) and the use of soil data that did not fully capture the variability of the alluvial deposits. Additionally, the program's versatility lets the user enter any number for end bearing and transfer skin friction as a function of depth (Reese et al., 2006).

Errors of up to 40% in bearing capacity and unrealistic failure modes were identified as major problems in analytical solutions (Picardo et al., 2023). The values obtained from the ASTM code for pile-bearing capacity generally agree with the results of static load tests in the field. The ASTM code specifies loading the piles up to 200% of the expected design load, applying loads in increments of 25% of the design load, and limiting movement to 0.25 mm (0.01 in) per hour. The results obtained from the ASTM code were found to be close to the field calculations. For example, the field-calculated load values for the first and second project piles were the same as those calculated based on the ASTM code. This shows a strong correlation between the values obtained from the ASTM code and the actual load-bearing capacity determined from the field static load test. Therefore, the ASTM code appears to provide a reliable and accurate estimation of the

History of article:
Received : 06 Juni 2024
Revised : 28 November 2025
Published : 31 Desember 2025

ISSN 2598-975 (Print)
ISSN 2598-8581 (Online)
ejurnal.poliban.ac.id

load-bearing capacity of the piles when compared to the results obtained from the field static load test. (Adel & Ressol, 2022).

E. Back Analysis of the Proposed Piled Raft

The chronology of why the piled-raft foundation is proposed is because the bearing capacity of piles resulting from static and dynamic tests does not meet the bearing capacity of the design. From the information above, the points that must be considered are sharing load (α_{PR}) and soil surface consistency or soil mechanical parameters that can support load sharing, for example, if soil consistency is loose, then sharing load (α_{PR}) according to Figure 1 must be limited to a maximum of 20%. An illustration of the proposed raft foundation can be seen in Figure 15 from the results of the structure calculation and pile load test results as follows:

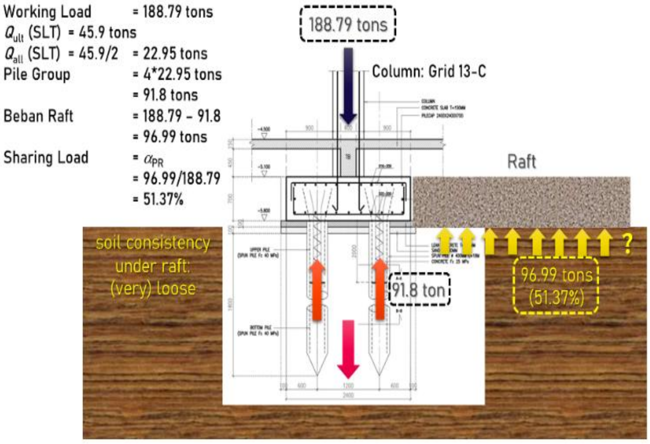

Figure 15. Raft Sharing Load ($\boldsymbol{\alpha_{PR}}$) on 13-C Grid Columns (Darjanto, 2024).

Based on the research results, the alternative solution offered by the PMCM and the contractor was to add a continuous foundation or raft with a thickness of 35 cm, which was considered too thin. Thinner rafts can lead to non-uniform loads borne by the piles, and the proportion of loads carried by the rafts is much higher than 20% and can be further adjusted by widening the spacing between piles (Yirsaw & Ashango, 2023). This is because, should the combined foundation system be used the load from the superstructure will be shared by the pile foundation and the piled raft can reduce the load per pile and the total settlement of the foundation. Therefore, the thickness of the raft plays an important role in influencing the settlement behavior of the piled raft system, with an optimal thickness being essential to achieving a balance between settlement and cost-effectiveness. (Ojha & Srivastava, 2023).

From a practical point of view, this case study highlights several lessons for similar projects:

1. analytical predictions of pile capacity should always be cross-checked against field load tests, especially where very loose surface soils and negative skin friction are present;
2. the use of soil data from nearby locations must be accompanied by sensitivity analyses to quantify uncertainty in key parameters; and
3. in piled-raft design for loose or soft deposits, the raft load share should be carefully limited and justified, rather than assuming a typical “standard” percentage, to avoid overstressing the near-surface layers and triggering excessive settlement.

The stiffness of piles and rafts greatly affects the load distribution in pile raft foundations. The load-sharing ratio of a pile raft foundation is affected by the stiffness of the pile and raft. By changing the stiffness represented by the dimensions of the pile and raft, the load distribution of the pile raft foundation can be modified under different scenarios. For example, increasing the thickness and dimension of the raft can reduce the number of piles in the pile raft foundation. The load-sharing ratio increases significantly with increasing raft thickness, especially in soft clay soil profiles. This indicates that the raft is more effective in carrying the load as the raft becomes stiffer (Mali & Singh, 2020).

From **Error! Reference source not found.** below, it is known that the total number of pile caps is 72, with each pile cap supporting 4 piles. Thus: $72 \times 4 = 288$ piles.

Meanwhile, the total allowable bearing capacity for all piles is: $72 \times 4 \times 225 = 64{,}800$ kN.

From the comparison in TABLE 7, the USACE and Revised Lambda methods provide the closest agreement with the SLT and PDA results, while the API and FHWA methods tend to be more conservative. For subsequent assessments in this study, the USACE/Revised Lambda range is therefore considered more representative of the local soil conditions, while the API/FHWA predictions are treated as lower-bound estimates.

TABLE 7. Calculated Axial Force

No.		Workload Total	Raft	Additional Piled
1.	Gravity Load	146,693.15 kN	$20\% \times 146{,}693.15$ $= 29{,}338.63$ kN	146,693.15 – 29,338,63 – 64,800 = 52,554.52 kN $= 52{,}554.52/225 = 234$ piles
2.	Nominal Earthquake Load	150,452.719 kN	$20\% \times 150{,}452.719$ $= 30{,}090.5438$ kN	150,452.719 – 30,090.5438 – 64,800 = 55,562.1752 kN $= 55{,}562.1752/225 = 247$ piles

History of article:
Received : 06 Juni 2024
Revised : 28 November 2025
Published : 31 Desember 2025

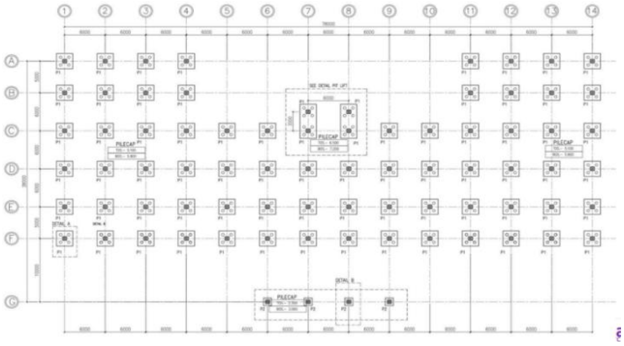

Figure 16. Pile Cap Plan (Darjanto, 2024)

The load-sharing ratio between piles and rafts in piled raft piles is influenced by several factors. These include the stiffness of the piles and rafts, the contact surface area of the rafts and piles with the ground, the dimensions of the piles and rafts, and the bearing capacity of each component. In addition, the size of the raft and the number of piles provided also affect the load-sharing ratio. The innovative design approach considers the combined action of pile and raft foundations, which results in an increased load-bearing capacity of 175% to 600%, depending on the size of the raft and the number of piles provided (Raut et al., 2023).

F. Liquefaction Analysis

Should be noted that most of the soil types in the research area are loose to very loose (see Figure 17). There is a thin layer of clay and silt along the sand layer fraction. These conditions can increase the potential for soil to flow when liquefaction occurs. Flow liquefaction occurs when water-saturated cohesionless soils experience sudden vibrations or stress changes that cause an increase in pore water pressure and a decrease in effective stress to zero. As a result, the normally solid soil material changes its behavior to that of a liquid. This can cause the soil to destabilize and flow, often with very destructive impacts (Darjanto, 2018).

Figure 17. Loose – Very Loose Soils (Darjanto, 2018).

The liquefaction potential of a soil deposit is influenced by several factors that have been identified through laboratory investigations and field performance observations. These factors include soil type, where soils with a uniform grain size distribution are more susceptible to liquefaction than well-graded soils. Relative density or void ratio also plays an important role; loose sand can liquefy under certain conditions, whereas denser sand cannot. The initial confining pressure increases the pressure required to initiate liquefaction under cyclic loading, thus decreasing the liquefaction potential. The intensity of ground motion, which is related to earthquake shaking, as well as the duration of ground shaking, which determines the number of significant stress or strain cycles, also affect susceptibility to liquefaction. These factors are very important in evaluating liquefaction potential during an earthquake (Seed & Idriss, 1970).

One of the limitations and weaknesses of the data used in this study is that the soil investigation point is not in the project area, but in its vicinity. This is because the project is located in a restricted area, making direct soil sampling impossible. Therefore, it is possible that the soil data used in this study does not represent the actual soil conditions at the project site. This may affect the results of the calculation of the bearing capacity of pile foundations and piled raft foundations. To overcome this, it is recommended that measurements and observations of the groundwater level at the project site be carried out periodically, as well as load tests on pile foundations and combined foundations to verify the calculation results.

IV. CONCLUSION

This study had two main objectives: to identify the causes of the bearing capacity failure of the existing pile foundation for a six-storey building in Dili, and to evaluate the design adequacy of a proposed piled-raft foundation under the local loose soil conditions.

First, the back analysis of soil data, SLT, and PDA tests shows that the failure of the original foundation is primarily due to insufficient axial capacity and excessive settlement of the pile group, rather than to liquefaction or isolated construction defects. The calibrated single-pile capacities range between about 450 and 900 kN, whereas the structural design assumed a capacity of at least 1000 kN per pile; in other words, the design demand was up to roughly 50% higher than what the pile–soil system can safely mobilise. Combined with negative skin friction in the very loose near-surface layers (NSPT < 5), this led to large settlements (of the order of 400 mm) and visible signs of bearing capacity failure.

Second, the evaluation of the proposed piled-raft system indicates that its performance is highly sensitive to the proportion of load carried by the raft. When the raft is assumed to carry more than about 20% of the total vertical load, the contact pressure in the upper loose layers approaches or exceeds their ultimate bearing capacity, and computed settlements exceed serviceability limits. By limiting the raft load share to approximately 20%, both the bearing capacity of the near-surface soils and the total

History of article:
Received : 06 Juni 2024
Revised : 28 November 2025
Published : 31 Desember 2025

ISSN 2598-975 (Print)
ISSN 2598-8581 (Online)
ejurnal.poliban.ac.id

settlement remain within the criteria of SNI 8460:2017 and within the range suggested by piled-raft design recommendations in the literature.

For design practice, the results underline the need to (i) ensure that soil investigation data are obtained as close as possible to the actual foundation footprint, (ii) explicitly account for negative skin friction in very loose or soft surface layers, and (iii) calibrate code-based capacity predictions against local SLT and PDA data whenever possible. In piled-raft design on loose alluvial deposits, the raft load share should not be treated as a fixed rule-of-thumb value but should instead be justified through project-specific back analysis and settlement checks.

This case study is subject to several limitations. Soil data were taken from nearby boreholes rather than directly below the building, liquefaction susceptibility was evaluated mainly by grain-size screening rather than a full CSR–CRR analysis, and the back analysis relied on one-dimensional empirical and semi-analytical methods rather than full 3D non-linear numerical modelling. In addition, the conclusions are based on a single project and should be complemented by further case histories in similar geological settings.

Despite these limitations, the study contributes to a better understanding of piled-raft performance in loose granular deposits by linking code-based methods and field tests in a documented failure case, quantifying the gap between design assumptions and actual pile capacity, and demonstrating that a raft load share of about 20% is a reasonable upper bound for safe piled-raft design under the investigated soil conditions in Dili.

REFERENCES

Adel, R. and Shakir, R. (2022). Evaluation of Static Pile Load Test Results of Ultimate Bearing Capacity by Interpreting Methods. *IOP Conf. Series: Earth and Environmental Science.* pp. 1-20. **URL:** https://doi.org/10.1088/1755-1315/961/1/012013

Burland J., Chapman, T., Skinner, H., & Brown, M. (2012). *ICE manual of geothecnical engineering Volume 2 Geothecnical Design, Construction and Verification*. London: ICE Publishing.

Darjanto, H. (2018), *Laporan Kunjungan ke Lapangan Terkait, Gempa Palu*. Kajian Gempa Palu Provinsi Sulawesi Tengah, Pusat Studi Gempa Nasional.

Darjanto, H. (2024). *Inception Report: Review Design of PNTL Highrise Building.* Dokumen Laporan Pekerjaan.

Febriansya, A., Iskandar, Suyono, A., Sholehah, N. A., & Handayani, N. (2022). Analisis Kebutuhan Kapasitas Piled Raft Studi Kasus Pegadaian Tower, Jakarta Pusat. *RekaRencana: Jurnal Teknik Sipil*, *08*(03), pp. 165-175. **URL:** https://doi.org/10.26760/rekaracana

Hakam, A. (2020). *ANALISIS PRAKTIS POTENSI LIKUIFAKSI*. Padang: Andalas Press.

Kronologia Problema Report. (2021). Shanghai Construction Group CO., LTD.

Li, P., Xia, Y., Xie, X., Wang, J., Wang, C., Shi, M., Wang, B., & Wu, H. (2024). Study on Vertical Bearing Capacity of Pile Foundation with Distributed Geopolymer Post-Grouting on Pile Side. Materials *MDPI*, *17*(398), pp. 1-21. **URL:** https://doi.org/10.3390/ ma17020398

Mali, S. & Singh, B. (2020). 3D Numerical Modeling of Large Piled-Raft Foundation on Clayey Soils for Different Loadings and Piled-Raft Configurations. *Studia Geotechnica et Mechanica*, *42*(1), pp. 1-17. **URL:** https://doi.org/10.2478/sgem-2019-0026

Mandolini, A., Laora, R. D., & Mascarucci, Y. (2013). Rational Design of Piled Raft. *SciVerse ScienceDirect*, *57*(2013), pp. 45-52. **URL:** https://doi.org/10.1016/j.proeng.2013.04.008

Mandolini, A., Russo, G., & Viggiani, C. (2005). Pile foundations: Experimental investigations, analysis and design. *INTERNATIONAL SOCIETY FOR SOIL MECHANICS AND GEOTHECNICAL ENGINEERING*, pp. 177-213. **URL:** https://doi.org/10.3233/978-1-61499-656-9-177

Mudher, Z.M. & Ibtehaj, T. J. (2025). PILED RAFT FOUNDATION: STATE OF ART. *Kufa Journal of Engineering.* 16(4), pp. 645-657. **URL:** https://doi.org/10.30572/2018/KJE/160438

Ojha, D. & Srivastava, R. K. (2023). Numerical Analysis of Piled Raft Foundations in Alluvial soil. *Journal of Mechanical and Construction Engineering*. *03*(002), pp. 1-11. **URL:** https://doi.org/10.54060/jmce.v3i2.25

Picardo, A., Millan, M. A., Galindo, R., & Alencar, A. (2023). Revisiting the analytical solutions for the ultimate bearing capacity of piles embedded in rocks. *Journal of Rock Mechanics and Geotechnical Engineering*, *15* (6), pp. 1506-1519. **URL:** https://doi.org/10.1016/j.jrmge.2022.11.012

Raut, J. M., Khandeshwar, S. R., Pande, P., & Bajad, S. (2023). *Physical Modeling and Analysis of Cast–In–Situ Reinforced Cement Concrete Piled Raft in Clayey Soil.* KSCE Journal of Civil Engineering, pp. 1-11. **URL:** https://doi.org/10.1007/s12205-023-0507-0

Reese, L. C., Isenhower, W. M., & Wang, S. (2006). *ANALYSIS AND DESIGN OF SHALLOW AND DEEP FOUNDATIONS*. New Jersey: John Wiley & Sons, Inc.

Seed, H. B. & Idriss, I. M. (1970). *A SIMPLIFIED PROCEDURE FOR EVALUATING* (Issue November).

SNI 1726: 2019. *Tata cara perencanaan ketahanan gempa untuk struktur bangunan gedung dan non-gedung.*

SNI 8460: 2017. *Persayaratan Perancangan Geoteknik.*

Structure Analysis Report. (2014). TECHSINDO

History of article:
Received : 06 Juni 2024
Revised : 28 November 2025
Published : 31 Desember 2025

ISSN 2598-975 (Print)
ISSN 2598-8581 (Online)
ejurnal.poliban.ac.id

Consultant.
Thompson, S. J. (2011). *Geology and Soils in Timor Leste*.
US Army Corps of Engineers. (1991). *Design of Pile Foundations.*
Yirsaw, G. M. & Ashango, A. A. (2023). *Numerical Study on Optimization of Piled Raft Foundation on Stratified Soil under Static Load.* Hindawi, pp. 1-11. **URL:** https://doi.org/10.1155/2023/4732353

History of article:
Received : 06 Juni 2024
Revised : 28 November 2025
Published : 31 Desember 2025